SPATIAL DISTRIBUTION OF BADLANDS IN THE UGUM WATERSHED: CHARACTERIZATION AND TEMPORAL ANALYSIS

By

Shahram Khosrowpanah
Yuming Wen
Maria Kottermair

WATER AND ENVIRONMENTAL RESEARCH INSTITUTE
OF THE WESTERN PACIFIC
UNIVERSITY OF GUAM

Technical Report No. 126
March 2010

SPATIAL DISTRIBUTION OF BADLANDS IN THE UGUM WATERSHED: CHARACTERIZATION AND TEMPORAL ANALYSIS

By

Dr. Shahram Khosrowpanah
Dr.Yuming Wen
Maria Kottermair

University of Guam
Water and Environmental Research Institute
of the Western Pacific
UOG Station, Mangilao, Guam 96923

Technical Report No. 126
March 2010

The activities on which this report is based were financed in part by the Department of the Interior, U.S. Geological Survey, through the University of Guam Water and Environmental Research Institute of the Western Pacific.

ABSTRACT

Soil erosion, rather common in the southern part of Guam, marks the savanna landscape in the form of erosion scars. These large, orange-red colored patches are often called badlands. Soil erosion not only degrades the quality of the topsoil, but also severely impacts the water quality in the streams and the ocean where it also affects the coral reef system and marine flora and fauna. Several studies (Khosrowpanah *et al.* 2007, Golabi *et al.* 2005, Scheman *et al.* 2002, Lewis 1999) have shown that badlands are one of the major contributors of soil erosion and associated sedimentation. Although several studies have measured erosion rates of badlands on Guam, the change of badlands through time as well as terrain attributes (that affect badland distribution) was unknown prior to our study. We utilized a geographic information system (GIS) to quantify temporal changes in badland coverage of a historical aerial image and up-to-date satellite imagery in our study area in the Ugum Watershed. In addition, we conducted a quantitative spatial analysis of badlands and their distribution to characterize badlands in respect to terrain attributes like elevation, slope, slope direction (aspect), distance to drainage divide, geology, and soils. Our results show that badlands have expanded over time, but they also have the ability to recover. More studies on badland change over time in other areas on Guam at a smaller time-interval are needed to more accurately determine the overall rate of badland change. We also found a significant relationship between proportional abundance of badlands and elevation, slope, distance to drainage divide, and soils. The relationships of the spatial distribution of badlands and terrain attributes provide the basis for future development of a predictive model for mapping potential badland areas on southern Guam.

KEYWORDS: Badlands, Geographic Information System, Ugum Watershed, Sedimentation

TABLE OF CONTENTS

LIST OF FIGURES

LIST OF TABLES

INTRODUCTION

Soil erosion creates several environmental problems for the island on Guam. Excessive soil loss degrades the quality of the topsoil and its ability to sustain agriculture. The detached sediment particles are transported by surface runoff to lower areas and eventually deposited into nearby rivers and other water bodies. The highly turbid water flowing into the ocean can damage the coral reef system, which is an important natural as well as economic resource for Guam.

In southern Guam, drastic soil erosion processes mark the savanna landscape in the form of large, orange-red colored erosion scars, so-called badlands (Fig.1). The countless red spots—as visible apparent on satellite imagery—are evidence for their vast existence throughout the southern watersheds. Badlands are continually eroding soils on steeply sloping terrain.

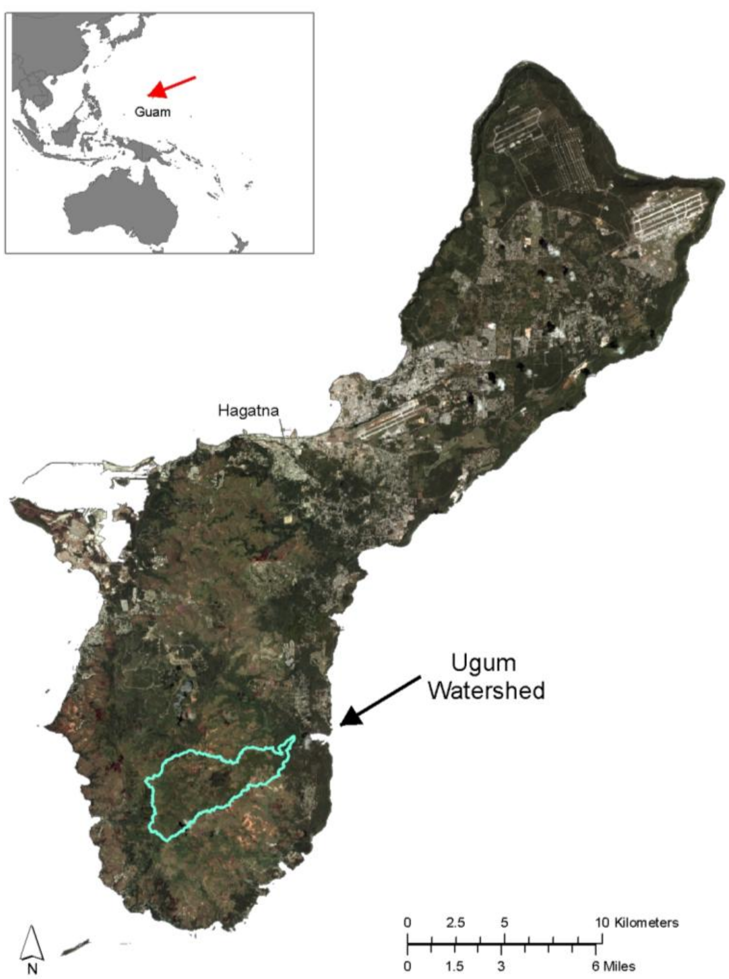

Figure 1. Satellite imagery of Guam with boundary of the Ugum Watershed on Guam.

Traditional field inventories and surveys may accurately delineate the boundaries of each badland area and associated terrain attributes, but it is very time-consuming and the areas are often hard to access. In addition, the extent of badlands has not been monitored in the field in the past and, therefore, makes a long-term badland change analysis using field data impossible. New technology such as remote sensing and geographic information systems (GIS) can overcome these challenges. Currently, Guam has several aerial coverages taken in different years, dating back to 1946. Earlier coverages were captured from airplanes on black-and-white film, while more recent multi-band images were acquired from satellites such as Landsat, IKONOS, and QUICKBIRD. Two images, a historical aerial photo from 1946 and a current satellite image from 2006, were utilized to analyze the extent of badland change over more than sixty years. The current satellite imagery and new terrain data (LiDAR) were further used as a basis to characterize topographic variables of badlands.

PROJECT GOALS

The primary goal of this project was to identify, map and analyze the changes in badland areas over time. In addition, the characterization of badlands in respect to topographic variables and structural pattern will be investigated. The secondary objective is to recommend appropriate soil erosion prevention strategies for critical areas. The specific goals are:

1. To compile an inventory of all available aerial images of Guam, including historical aerial photographs and recent satellite imagery, and select two suitable images for the badland change analysis.

2. To georeference the selected images in the geographic information system (GIS) software ArcEditor 9.1 and digitize the extent of badlands in both images. Further, to detect changes in badland cover over time via raster analysis.

3. To find a relationship of the current badland extent and topographic variables (elevation, slope, aspect, distance to drainage divide, geology, and soils) via frequency distribution to identify preferable conditions of badland formation; this process will be executed in the GIS extension Spatial Analyst and Microsoft Excel. To characterize the structural pattern of the badlands with the GIS-extension V-LATE.

4. To recommend appropriate soil erosion control practices and re-vegetation methods for the badlands.

RELATED RESEARCH

Badlands are found throughout the world and are not restricted to the humid climate. Much research has been done on soil erosion in general and badlands in particular, but studies mainly focus on erosion rates, not the change of badland extent over a long-term period. Few studies address the relationship between badlands and topographical variables like elevation, slope, and aspect (*e.g.*, Canton *et al.* 2004, Calzolari & Ungaro 1998, Lin & Ogushi 2004). Land cover change, which includes changes in erosion scars, has been studied extensively all over the world, including Italy (*e.g.*, Liberti *et al.*, 2006), Ethiopia (*e.g.*, Bewket, 2002), and Palau (*e.g.*, Endress, 2001). However, these changes are usually analyzed at a regional scale at a small resolution rather than a local scale at high resolution, thus they cannot detect relatively small-scale phenomena like the badland patches on Guam. Few badland studies have been conducted on Guam in the past decade, but they mainly concentrate on erosion rates.

Related Modeling Studies on Guam

A GIS-based soil erosion model of the Ugum watershed has been developed by Khosrowpanah et al. (2007). The model combines the Universal Soil Loss Equation (USLE) with the capabilities of GIS to identify the maximum potential rate of soil loss within the entire Ugum watershed at a 10 meter resolution. The greatest erosion potential lies in badlands and in areas with steep slopes (> 30 degrees). The highest estimated computed soil erosion potential is 1,172 tons/ha/yr. Studies by the Natural Resources Conservation Service (NRCS) estimated that badlands contribute a sediment loss of 243 tons/acre/year in the Ugum Watershed (NRCS, 1996), 240 tons/acre/year in the Fena Watershed (NRCS, 2001), and 130 tons/acre/year in areas with 30–60 percent slopes in Sella Bay and Cetti Bay (NRCS, 2006).

A quantitative land cover change study for southern Guam was conducted by Wen (2009). Land cover was derived from multi-date satellite Landsat imagery from 1973 (the oldest available satellite imagery for Guam) and 2001. The resolution of the Landsat imageries is less than 30 m x 30 m which is suitable for a large scale land cover change analysis of southern Guam, but not for fine-scale changes focused on badlands like in this analysis.

Another land cover change project is the Coastal Change Analysis Program (C-CAP) by the National Oceanic and Atmospheric Administration *(*NOAA*)* Pacific Services Center (Carter 2009). This project, based on the 2006 multi-spectral QUICKBIRD imagery with a 2.4-meter resolution, provides detailed information on the location and extent of man-made impervious surfaces and other land cover. A goal of C-CAP is to map the coastal areas every five years to detect changes in land cover due to human and natural impacts (Carter, 2009).

Khosrowpanah *et al.* (2008) developed a digital watershed atlas for southern Guam. The area covered in this online resource database—including physical, environmental, and socio-economic baseline information—contains fourteen watersheds. The atlas can be viewed and data in various formats can be downloaded at http://www.hydroguam.net. A soil and geologic layer file from this database has been utilized for this study.

Badland Field Studies on Guam

The Ugum watershed is one of the most studied watersheds on Guam. Various reports are available: Botanical Survey of the Riverine Forest (Rinehart, 1995), Wetland Resource Assessment (Siegrist *et al*,. 1996), Non-point Source Pollution Assessment (Khosrowpanah *et al*., 2005), Ugum Watershed Restoration Strategy (WPC, 1999), and Ugum Watershed Management Plan (NRCS ,1996).

Few studies addressing badlands in particular have been conducted on Guam. Lewis (1999) investigated sediment yield, slope retreat, and fracture movement in four individual badland basins within the Taelayag Watershed in southern Guam. The study revealed erosion rates ranging from 2.1 to 9.5 tons/acre/year for badlands. Although the erosion rate is lower than expected, the impact of badland erosion is still significant (Lewis, 1999).

Scheman et al. (2002) empirically measured erosion rates of badlands with different slopes in the La Sa Fua Watershed. They compared their results with erosion rates calculated using the Revised Universal Soil Loss Equation (RUSLE) and found that RUSLE consistently overestimated the erosion rates measured in their study. As expected, the highest average erosion rate occurred in the badlands. The soil loss at the different test sites (badlands and grasslands) is equally connected to slope angle, but barren soil exhibits a stronger relationship with precipitation accumulation than soil in grasslands. Subsequent a typhoon, erosion increased in the steep badland areas. Scheman et al. (2002) concluded that various topographic and climatological factors may influence the development of badlands. By means of a time-series photograph (one year apart) they also showed that the number of badlands is increasing.

Golabi et al. (2005) studied the effects of different soil surface conditions on water quality in southern Guam. The runoff from four different plots (natural savanna vegetation, vetiver system, controlled burn, bare soil) was tested for sediments and turbidity. The vetiver system proved to be very successful in trapping sediments, but also in improving the water quality. The plot with no vegetation cover—representing badlands—showed by far the highest amount of sediments and turbidity values. The overall projected soil loss for barren soil was more than seventy-fold (104.75 tons/ha/yr) that of vetiver system (1.47 tons/ha/yr); the natural condition (savanna) lost three times more soil and the burned plot lost about ten times more than the vetiver system treatment. The researchers recommend the vetiver system with its distinctive characteristics for soil erosion control and restoration of natural resources.

The National Park Service is currently investigating the effects of four-wheeling on the development on badlands in the Mt. Tenjo National Historic Park (Capone 2008, pers. comm.).

The completed field studies (Lewis 1999, Scheman *et al.* 2002, Golabi *et al.* 2005) clearly show that the overall erosion rate in badlands is much higher than in any other type of vegetation cover. The erosion potential models (NRCS 1996, Khosrowpanah 2007), although highly overestimating actual erosion rates (see above), confirm the results of the field studies.

All the above mentioned research focuses on erosion rates and soil losses in badlands and other vegetation covers. Very little literature concerning badland formation on Guam is available. In their textbook “Tropical Pacific Island Environments”, Lobban and Schefter (1997) dedicate one section to badland formation. They attribute factors like fires or overgrazing, exotic grass species, erosion, and certain soil characteristics to the formation of bare areas in the Pacific.

However, no studies address the actual behavior of badlands on Guam besides erosion rate. A study regarding the change over time of these eroded areas as well as their terrain attributes is much needed to better understand and, hence, manage these landforms. The ultimate goal is to reduce the detrimental effects of erosion of Guam’s uplands and sedimentation of the reefs.

Studies from other Countries

Canton et al. (2004) studied influence of terrain attributes on the spatial distribution of ground cover, including bare marl regolith, in the Tabernas badlands of SE Spain. They found that local terrain attributes (*e.g*., slope angle, aspect, and elevation) have a greater influence on ground cover types than non-local terrain attributes (contributing area, wetness index, length slope factor). The relationship of aspect and slope length and erosion rates did not show a significant relationship, whereas erosion rate peaked at slope angles of 3 –45 degrees (Clark and Rendell, 2006). Torri *et al.* (1994) noted that badlands (*biancana*) in Italy are mostly established in slopes up to 30–50 percent. The genesis and evolution of calanchi badlands in Italy is attributed to the interaction of highly erodible soils and substrate, climatic factors, and agricultural and tectonic activity (Moretti *et al.*, 2000).

Historic aerial photographs have been used to track environmental changes in the past. These photographs are often oblique (horizontal distortion created b y camera angle) and, therefore, pose a challenge to rectify, which has not been fully resolved to date (Levesque, 2000).

OVERVIEW

Study Area

Guam is the largest and southern-most island of the Mariana Archipelago in the Western North Pacific. The elongated island is about 30 miles (48 km) long and between 4 to 9 miles (7-15 km) wide with a total area of 212 square miles (549 km^2). It is bordered by the Pacific Ocean to the east and the Philippine Sea on the west. The Mariana Trench passes Guam about 250 miles (400 km) southwest of Guam.

Figure 2. Aerial view of southern Guam. Light-red patches (see arrows) are badlands**.**

The Ugum Watershed encompasses a 7.3 square miles area located along the eastern coast of southern Guam (144°42'E, 13°18'N). The study area is a sub-watershed of the Talofofo watershed, the largest drainage system on southern Guam (Fig. 3). The Ugum Watershed includes a 23 miles stream network with two main rivers, the Ugum and Bubulao River. The Bubulao River drains into the Ugum River, which merges into the Talofofo River near the outflow to Talofofo Bay. The elevation of the Ugum Watershed ranges from 6 m (20 ft) to 374 m (374 ft) with an overall relief of about 368 m (354 ft).

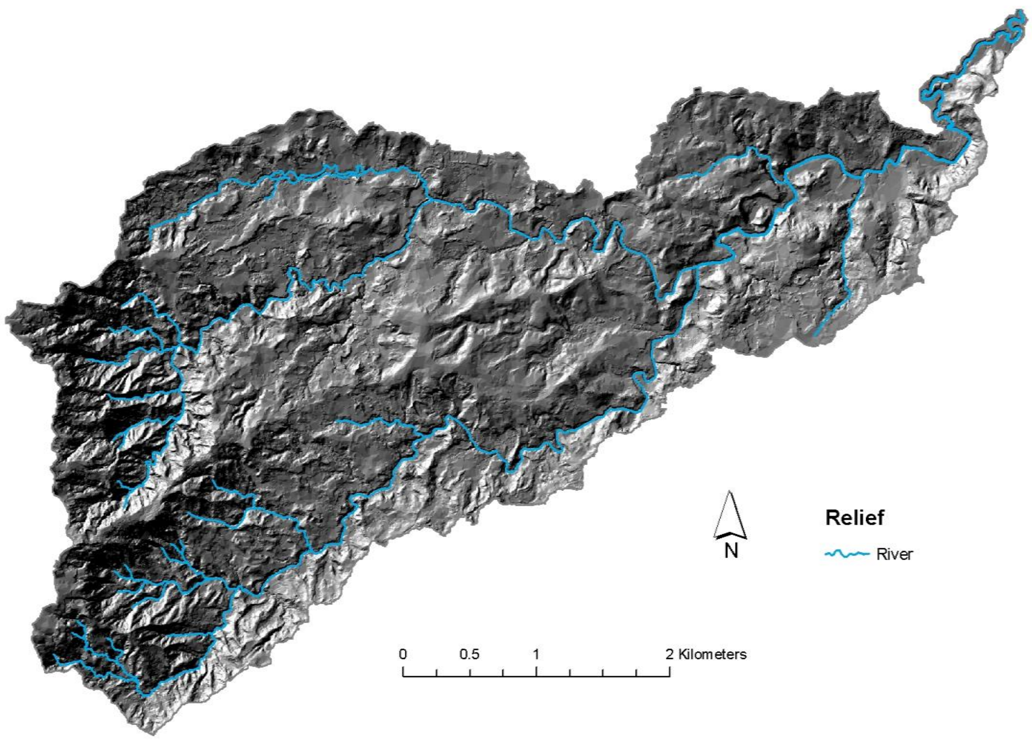

Figure 3. Hillshade with rivers of the Ugum Watershed.

Climate

Guam has two distinct seasons, a dry (January-June) and a wet season (July-December). The mean annual temperature is 81 degrees Fahrenheit, with little seasonal variation. Depending on the topography the annual mean rainfall on the island ranges from 85 inches to 115 inches, whereas about 70% of rain falls during the wet season (Lander & Guard, 2003). The inter-annual variability of Guam's rainfall is strongly related to the irregular recurrence of episodes of El Nino Southern Oscillation (ENSO) (Lander, 1994). The year following El Nino is usually very dry (Lander & Guard, 2003). The annual rainfall distribution maps for Guam show strongest rainfall gradients along the western and southern mountains (Lander & Guard, 2003) where our study area is located at. During the wet season the island has prevailing southeast winds (or strong southwest winds during occasional monsoons); during the dry season prevailing trade winds, predominantly from east-northeast (Lander 2009, pers.comm.). Guam is also frequently subjected to tropical cyclones because of its location in the world's most active ocean basin (Lander, 1994). During the period 1945-2007, 183 tropical cyclones (maximum sustained winds ≥ 34 knots) passed within 180 nautical miles (nm), with 75 that reached typhoon intensity (Kottermair and Olsen, unpubl.). Although only passing by shortly, tropical cyclones contribute about 12% to Guam's average annual rainfall (Lander, 1994). During a direct eye passage of a typhoon the island experiences extremely high short-term rainfall rates that can exceed 18 cm an hour as encountered during Typhoon Pongsona in 2002 (Lander & Guard, 2003).

Geology

Guam is divided into two distinct geologic zones separated by a major fault zone stretching from Adelup Point to Pago Bay in central Guam. The northern half of the island is comprised of a limestone plateau with an underlying volcanic rock that protrudes to the surface at Mount Santa Rosa and Mataguac Hill. Due to the high permeability of the limestone precipitation infiltrates almost instantaneously into the ground, allowing no rivers to form. Contrary to the elevated limestone plateau with steep cliff, the southern part is primarily of volcanic origin with some peaks and ridges capped by limestone. The terrain is characterized by dissected volcanic uplands and extensive stream network. The three volcanic formations that build the base of the island are Facpi, Alutom, and Umatac Formation. Facpi, the oldest formation dating back to the Eocene, underlies the Umatac Formation over most of the southern part of southern Guam.

Almost the entire study watershed is classified as the Umatac Formation. Most of the formation belongs to the Bolanos Pyroclastic Member with small patches of the Dandan Flow Member, remnants of the last volcanic eruption during the Miocene age. The Bolanos Pyroclastic Member consists of thick-bedded to massive tuff breccia, thin-bedded tuffaceous sandstone, and lenses of volcanic conglomerate (Tracey *et al.* 1964). The tuff breccia is a conglomerate of basaltic and andesitic rock, tuffaceous shale, and Maemong Limestone fragments in a sandy tuffaceous matrix (Tracey *et al.* 1964). Tuffaceous sandstone is prevalent in the dissected uplands between Ugum and Inarajan River and exposed in badlands (Tracey *et al.* 1964). On the east coast the Bolanos Pyroclastic Member is overlain by the Hagåtña Argillaceous Member of the Mariana Limestone

Soils

Soils generally follow the bedrock; hence limestone soils are mainly found in the north whereas volcanic soils in the south. Young (1988) delineated 25 map units based on nine difference soil series and slopes within Ugum Watershed. The various soils are Agfayan, Akina, Atate, Badlands, Inarajan, Pulantat, Sasalaguan, Togcha, and Ylig group. Badlands are actively eroding areas of very deep and well drained saprolite developed from tuff and tuff breccia, usually with little or no vegetation; slopes are short, irregular, and can vary from a moderate angle to vertical (Young, 1988). The color of the badlands ranges from a rich red or even purple to orange and white. Due to the relatively slow permeability of the saprolite, rain drains overland as runoff, leading to severe soil erosion.

Land Cover

Based on a 2002 IKONOS satellite imagery classification (Donnegan *et al*. 2004), the island is covered with 48 percent forest, one third grass and shrublands, 18 percent urban areas, and one percent barren lands. The forested area is comprised of approximately 70 percent limestone and thirty percent volcanic/ ravine forest. Guam's present vegetation is a result of several factors including tropical cyclones, arson, erosion, invasion of introduced weeds and feral ungulates, past military actions and logging (Donnegan *et al.*, 2004).

The vegetation of the southern, volcanic part of Guam is characterized by a mix of grassland (savanna) and patches of forest, which generally follow topographic features like river drainages, sheltered depressions, and ravines (Donnegan *et al.*, 2004). Bell *et al.* (2002) describe the savanna grasslands as a mosaic of *Miscanthus* grasslands *(Miscanthus floridulus,* sword grass*)*, badlands, *Dimeria* and mixed grass lands (primarily *Dimeria chloridiformis*, an endemic tuft grass found in more level areas), *Phragmites* wetlands (*Phragmites karka,* found in water-logged area), and savanna shrub lands.

Land Use

The majority of the Ugum watershed (70%) today is owned by the public and the remaining by 15 private landowners (Khosrowpanah *et al*., 2005). The western area of the drainage basin is part of the 2,854 acres (11.6 km^2) Bolanos Conservation Reserve and under the stewardship of the Division of Aquatic and Wildlife Resources. The privately owned land is classified as "Agricultural Zone", but most of it is undeveloped; only 1.2 % (Khosrowpanah *et al*., 2005) is cultivated during the dry season. Erosion problems resulting from agricultural activities in this area are considered minor (Khosrowpanah *et al*., 2005). Two paved roads exist within the boundary of the watershed. One leads to the Ugum River water intake, the other to the "Talofofo Falls Park" which includes a gondola, museum and gift shop.

The main recreational activities within the Ugum watershed are hiking, hunting, and off-roading (Khosrowpanah *et al.*, 2005). Most wildfires are associated with arson set by hunters. The intention is to attract deer that is drawn to the new grass shoots following wildfire. Wildfire has an impact on erosion and species composition as mentioned above. In addition to wildfire, off-roading (four-wheel driving) is also believed to be a major contributor to erosion by expanding badlands and other erosion-prone land cover types (Porter *et al*., 2005). Off-roading can damage vegetation and/ or loosen soil leading to increased soil erosion.

METHODOLOGY

Badland changes in our study in southern Guam were quantified using a spatial overlay analysis of aerial imagery from 1946 and 2006 in a geographic information system (GIS), ArcGIS 9.2 Spatial Analyst extension. The analysis was based on a geo-referenced historical aerial photograph and recent QUICKBIRD satellite imagery. The characteristics of badlands were assessed by means of a structural pattern analysis and a frequency analysis with various layers. The latter was used to investigate possible relationships of badlands with topographic controls like elevation, slope, aspect, and distance to drainage divide.

Data Sources

Imagery

We inventoried available aerial and satellite imagery to find two images from different years suitable for a time-series analysis of badlands (see Table 1). The oldest available panchromatic (black-and-white) aerial image series dates back to 1946, whereas the most recent satellite image was taken by QUICKBIRD satellite in 2006. The first color satellite image was taken by LANDSAT in 1973 with a resolution of ~ 80 m x 80 m. The aerial photos were all evaluated regarding overall clarity, resolution, badland identification, and cloud cover. The 2006 QUICKBIRD and the 1946 Aerial Photo, spanning over a sixty year period, were determined the most suitable (Fig. 4).

The 2006 QUICKBIRD (QB06) imagery was taken between 21 May 2005 and 31 March 2006 by Digital Globe for U.S.D.A. Natural Recourses Conservation Service. The QB06 is a 4-band (blue, green, red, and Near IR), pan-sharpened digital orthoimage with a 0.6 m x 0.6 m ground resolution, projected in Universal Transverse Mercator Zone 55N with a WGS 1984 datum. No adjustments were necessary for this imagery.

The oldest available historic aerial photographs were acquired 1 February 1946 using panchromatic film. A total of 58 photos represent several passes over the island. Hardcopies of this series are part of the Micronesian Area Research Center (MARC) Collection at the University of Guam. MARC scanned the images at 600 dpi resolution. The images are considered low-angle oblique aerial photographs, meaning that camera axis was not truly vertical at the time of exposure, but the horizon is not visible. Consequently, the scale is not constant over the extent of a single photograph. In contrast, an orthophoto is a planimetrically corrected aerial photograph where the distortions caused by the terrain and camera angle and lens have been removed. An orthophoto combines the characteristics of a digital image with the geometric qualities of a map. However, due to the lack of camera calibration an ortho-rectification of the historical aerial photographs could not be performed for this study.

Table 1. Inventory of available aerial imagery on Guam.

Name	*Year*	*Area Covered*	*Date taken*	*Format*	*Sheets*	*Resolution*
QUICKBIRD	2006	Whole Island	May 05 - Mar 06	digital		0.6 m x 0.6 m (pan-sharpened)
	2005	Whole Island	Nov 03 - Feb 05	digital		
IKONOS	2004	Whole Island	Nov 02 - Jan 04	digital		4 m x 4 m
Landsat	2000	Whole Island		digital		
	1974	Whole Island		digital		
Aerial Ortho-Photos	1993	Whole Island	1992 - 1994	hardcopy, digital		
Aerial Photos	1986	North	1985 - 1986	hardcopy, scans	55	
	1975	Whole Island	5/30/1975 - 7/8/75	hardcopy, scans	91	
	1974	Whole Island		hardcopy - ca. 22 x 34		
	1973	Agat, Tamuning	24-Aug-73	hardcopy, scans	58	
	1970	Central	4-Jun-70	hardcopy, scans		
	1969	North, Central	26-Jan-69	hardcopy, scans	90	
	1964	Whole Island		hardcopy, scans	115	
	1964	North	30-Mar-64	hardcopy, scans	53	
	1956	Whole Island	12-Mar-56		38	
	1953	Whole Island	26/28-Jan-53	hardcopy, scans	191	
	1946	Whole Island	1-Feb-46	hardcopy, scans	58	600dpi

For this time-series analysis, we chose the image inscribed “GC12B.83-VV-3RS-M-30ENG-1FEB46-MI” (further called “AP46”) covering a large part of the Ugum Watershed was chosen. Although other images also depict the study area, they only show it on the edge of the photograph where the distortion is the greatest. For this reason, a smaller area within the study area was selected.

Using the geographic information system (GIS) software ArcGIS 9.1, we rectified the GC12B.83 image three times. Each time we focused the ground control points (GCPs) on a different area (“frame”) of the image to minimize the root mean square error (RSME). We chose 40, 20, and 19 GCPs, respectively, for each frame. The GCPs were derived from the 2006 QUICKBIRD satellite imagery. Due to the lack of streets or structures and other readily visible natural features like rivers, distinctive forms of badlands represented in both imageries served as references for the GCPs. We used a third-order polynomial transformation for all three frames, with a total RMS Error of 1.85 m, 1.89 m, and 1.96 m, respectively. The images were resampled to a cell size of one meter using the bilinear interpolation method and saved as an IMAGINE image format. The resampled images were then clipped to their respective frame and photo-mosaicked to one single file.

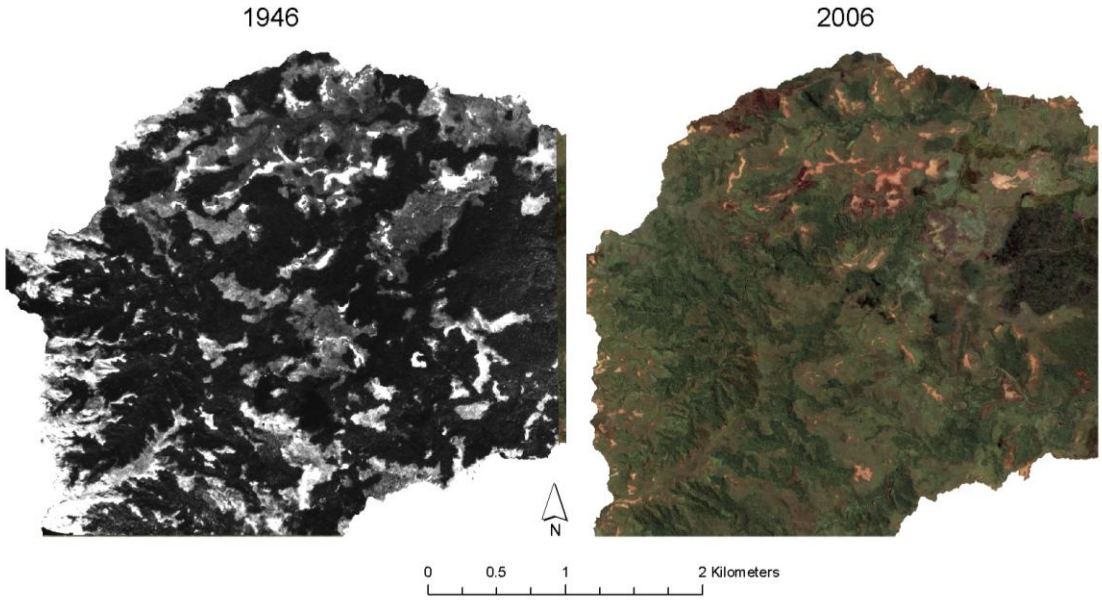

Figure 4. Georeferenced aerial imagery (1946) and QuickBird satellite imagery (2006) of study area.

LiDAR

Light Detection and Ranging (LiDAR) is a remote sensing system used to collect topographic data of the earth's surface. The LiDAR sensor (*e.g.* mounted on an aircraft) sends out narrow, high frequency laser pulses toward the earth and records its travel time. From the time difference between emission and return of the signal and the exact position through a high–precision global positioning system (GPS), a Digital Elevation Model (DEM) of the ground surface can be generated.

LiDAR data for Guam was collected for the Government of Guam Department of Public Works and Homeland Security between February and May 2007. At the time of this analysis only draft LiDAR data was available. However, due to the high accuracy of the LiDAR data (compared to the currently used 10-m resolution DEM by USGS) we utilized the draft LiDAR to derive watershed boundaries, slope, aspect, and elevation. We derived the watershed boundaries from the LiDAR data (5-m resolution) by running Arc Hydro Tools, an ArcGIS extension jointly developed by the Center for Research in Water Resources (http://www.crwr.utexas.edu) of the University of Texas at Austin and the Environmental Systems Research Institute Inc. We extracted terrain information—elevation, slope, and aspect—with the ArcGIS 9.2 extension Spatial Analyst Surface Tool for *Aspect*, *Slope*, and (for visual purposes) *Hillshade*.

Badland Delineation

The extent of badlands in 1946 was derived by extracting all pixels from the 1946 rectified image (AP46) with values between 150 and 255 (on a Grayscale 0–255). The values were determined through visual examination trying to capture all highly reflective areas thought to be badlands. We reclassified the layer by assigning a value of "1" for "badland" and "0" for "not badland".

The extent of badlands in 2006 (length > 7 m) was digitized by hand based on the 2006 QUICKBIRD imagery (QB06). However, a vegetation layer for the whole island (derived from the 2004 IKONOS imagery) exists, but the resolution was too low and classification of badlands too inaccurate for our study. After digitizing the badlands, we converted the badland polygons to a one-meter–resolution raster and reclassified the layer by assigning a value of “10” for “badland” and “0” for “not badland”.

Badland Change

To investigate badland change between 1946 and 2006, raster layers AP46 and QB46 were evaluated together using the mathematical function *Addition* in the Raster Calculator. The outcome layer contained four categories: areas that were not badland in either year [value: “0” (“0 +0”)); badland in 1946 only [value: “1” (0 + 1)]; badland in 2006 only [value: “10” (“0 + 10”)]; and badland in both years [value: “11” (“1 + 10”)].

Structural Pattern Analysis

A structural pattern analysis revealed the number, sizes, and distances to closest neighbor of the 2006 badlands. For this analysis we used the GIS Vector-based Analysis Tools Extension V-LATE developed by the Landscape and Resource Management Research Group (LARG, 2005).

Badland Relation to Terrain Attributes

To assess the influence of terrain attributes on badlands, we analyzed the frequency distribution of badlands at specific intervals of elevation, slope, aspect, distance to drainage divide, geology, and soils and compared each of them to the corresponding frequency distribution of the entire watershed. The elevation, slope, aspect, and distance to drainage divide data were derived from LiDAR data; the geology (Tracey *et al.*, 1964) and soil data (based on Young 1988) were downloaded from the Natural Resources Atlas of Southern Guam website (Khosrowpanah *et al*., 2008). The frequency distributions were calculated with the Spatial Analyst Tool *Zonal Statistics* and evaluated in a spreadsheet.

Possible Sources of Inaccuracies

The delineation of badlands in both datasets (1946 and 2006) may have deficiencies in terms of ambiguity in interpretation. The rectification of the 1946 aerial photo may have several errors due to the inherent property of oblique photographs, and thus we cannot assess the true badland outlines in 1946. Also, the current badlands were not ground-truthed. The qualities of the source layers like LiDAR data, soil and geology were not verified.

RESULTS & DISCUSSION

Badland Change

Figure 5 shows the spatial distribution of badlands in 1946 and 2006, differentiating between areas that were badland (and non-badland respectively) in both years and areas that were badland in either 1946 or 2006, hence areas where badland change occurred within the last 60 years. Our study area covered ~ 60 percent (1105.78 ha) of the Ugum Watershed (1837.6 ha). The majority of the study area (92.72 %) was vegetated in both years while an area of 2.08 percent was classified as badland in both years (Table 2). An area of 1.32 percent (14.67 ha) within the study area has converted to badland since 1946, resulting in a total of 3.40 percent (37.65 ha) of badlands in 2006 (Table 3). In contrast, an area of 3.88 percent (42.85 ha) of the study area was classified as badland in 1946 but is now not badland anymore (mostly in the southwest corner); however, this number should be lower.

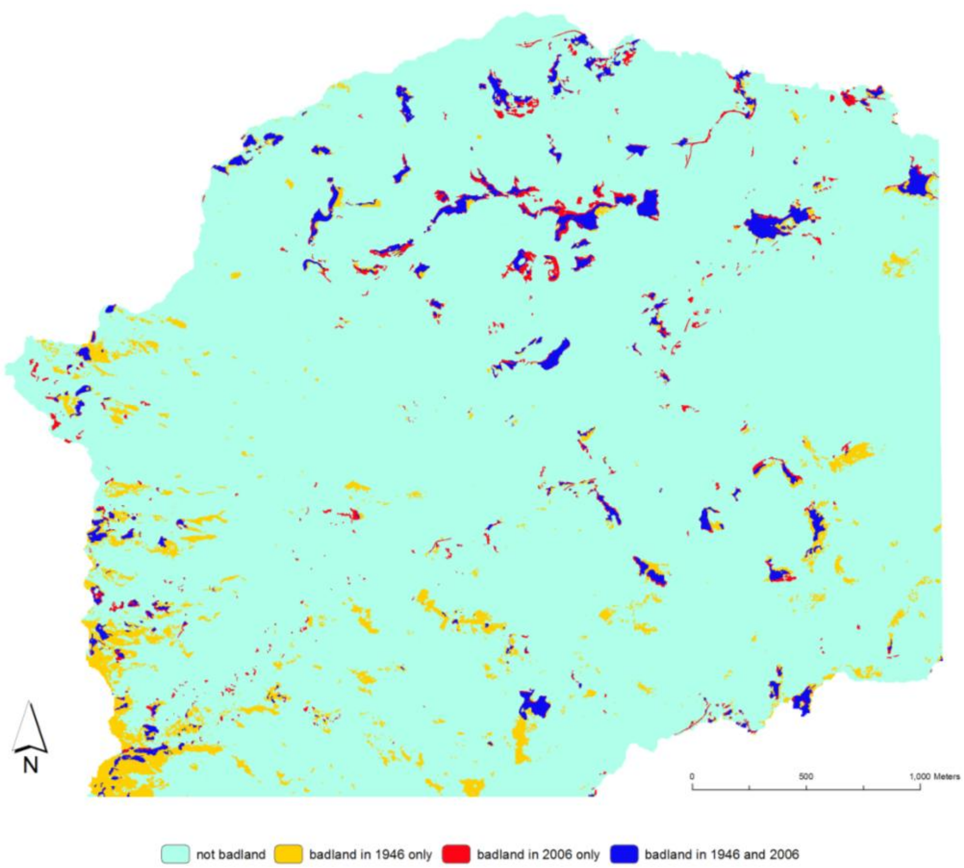

Figure 5. Badland changes between 1946 and 2006. The light-blue and dark blue areas indicate no change (not badland or badland in both years, respectively); the orange and red areas indicate change (badland in either 1946 or 2006, respectively).

Table 2. Statistical breakdown (in ha and percent) of areas that were not badlands in 1946 and 2006, badland in 1946 only, badland in 2006 only, and badland in 1946 & 2006.

Type	ha	%
Not badland in 1946 or 2006	1025.28	92.72
Badland only in 1946	42.85*	3.88*
Badland only in 2006	14.67	1.32
Badland in 1946 & 2006	22.98	2.08
Total Study Area	1105.78	100

* erroneous due to misclassification

Table 3. Total area in ha and percent of badlands and other land cover in 1946 and 2006.

	Badland		Other Land Cover		Total Area (ha)
	ha	%	ha	%	
1946	65.82*	5.95*	1039.96	94.05	1105.78
2006	37.65	3.40	1068.13	96.60	1105.78
Change	-28.17*	-2.55*	28.17	2.55	-

* erroneous due to misclassification

A comparison of the change analysis with the original (not georeferenced) historical photograph revealed that most badlands in the southwest corner were misclassified. The classification of the badlands in 1946 was based on pixel values of the georeferenced photograph; during georeferencing (when the original image is re-sampled) areas with greater distortion (in our case, the southwest part of the photograph) were contracted more than less distorted areas, resulting in non-linear converted pixel values (over the entire photograph) in the georeferenced photograph. In addition, the southwest corner of our study area coincides with the bottom edge of the photograph, which is brighter (like all edges of this photograph) than the interior. Therefore, badlands in areas with less distortion and in the interior of the photograph are represented well with our classification method, whereas badlands in areas with higher distortion and closer to the edge (southwest corner) were over-classified. Because of this error, the net change of badland area between 1946 and 2006 —which is negative according to our analysis— does not correspond to the visual interpretation of the images, which indicates a positive net change of badland area, and is thereby considered incorrect. Further observations are based on the northern (upper part) of the study area.

Our results demonstrate that badlands are dynamic. Larger badland patches (greater than ~ 70 m in length) are generally older than 60 years. They have expanded slightly to moderate over the years, while some decreased over the years—not taken into account the questionable large badlands in the southwest corner of our study area. However, these processes—expansion or contraction—are often observed in the same badland patches: some parts expanded while others contracted. Badland patches have also increased in numbers since 1946, although we were unable to determine the number of new badland patches with our pixel-based approach. Yet, it appears that badland patches also have the ability to recover and to sustain plant cover again.

Our time-series analysis focused on badland patches longer than 7 m and denuded of any vegetation. However, areas with only sparse vegetation or small patches (length < 7 m) of badland are a common landscape feature evident in the 2006 imagery. They seem to have increased largely since 1946 and, therefore, pose a serious erosion problem as they are likely converted to badlands in the near future.

Badland Structural Pattern Analysis

The total number of badland patches (< 7 m in length) in the entire Ugum Watershed in 2006 (based on the digitized badlands) was 819. The mean patch size is 673.8 m^2, but varies widely—between 5.6 m^2 and 25042.9 m^2 (Table 3). The majority of patches (85 %) is smaller than 1,000 m^2, only 14 percent are between 1,000 m^2 and 10,000 m^2, and less than one percent is larger than 100,000 m^2 (Fig. 6). The mean perimeter of a patch is 129.5 m. Larger patches seem to vary greater in perimeter, exhibiting highly complex elongated forms while smaller patches are generally more uniform (often oval) and have fewer indentations. The mean distance to the nearest neighbor is 20.1 m; the most isolated badland patch is within 246.5 m of another patch.

Table 3. Structural pattern characteristics of badland patches in 2006, Ugum Watershed, Guam.

Year	Number of patches	Mean	SD	Min	Max	Sum
Area (m^2)		673.8	1832.3	5.6	25042.9	553849.7
Perimeter (m)	819	129.4	195.7	8.8	2103.6	105981.8
Distance to NN (m)		20.1	28.8	0	246.5	-

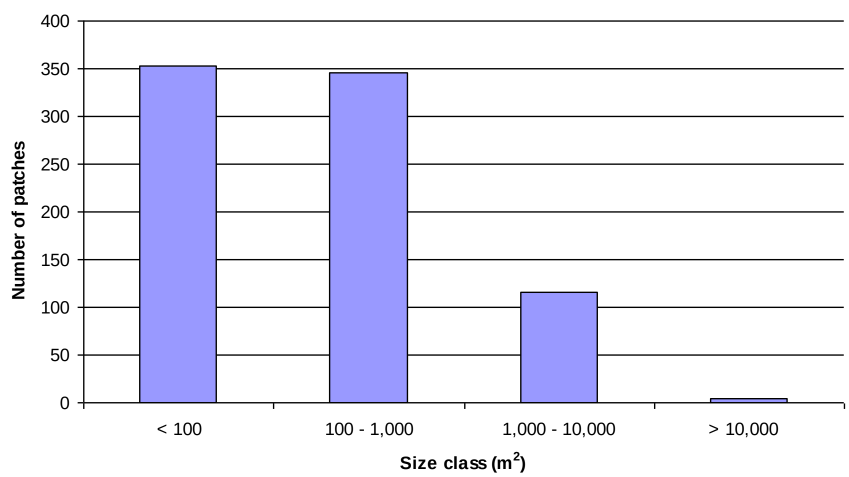

Figure 6. Frequency distribution of the area of badland patches (n =819) in 2006, Ugum Watershed.

Terrain Attributes

Badland – Elevation Relationship

The elevation in the Ugum Watershed ranges from ~ 0 m at the confluence of the Ugum and the Talofofo River to ~ 378 m in the mountainous interior (Fig. 7). Almost three-fourths of the watershed is less than 150 m above mean sea level (Table 4). Badlands cover a total of 3.01 percent of the watershed. More than half of all badland areas (56.3 %) have an elevation of 100–150 m and another 20.3 percent have an elevation of 50–100 m. However, the proportional abundance of badlands per elevation category (how much of a category is covered by badlands) shows that badlands are most frequent above 300 m but also have a high presence between 100–150 m (Fig. 8). The relationship between badlands and elevation is not linear; *e.g*., relative frequency of badlands increases with elevation.

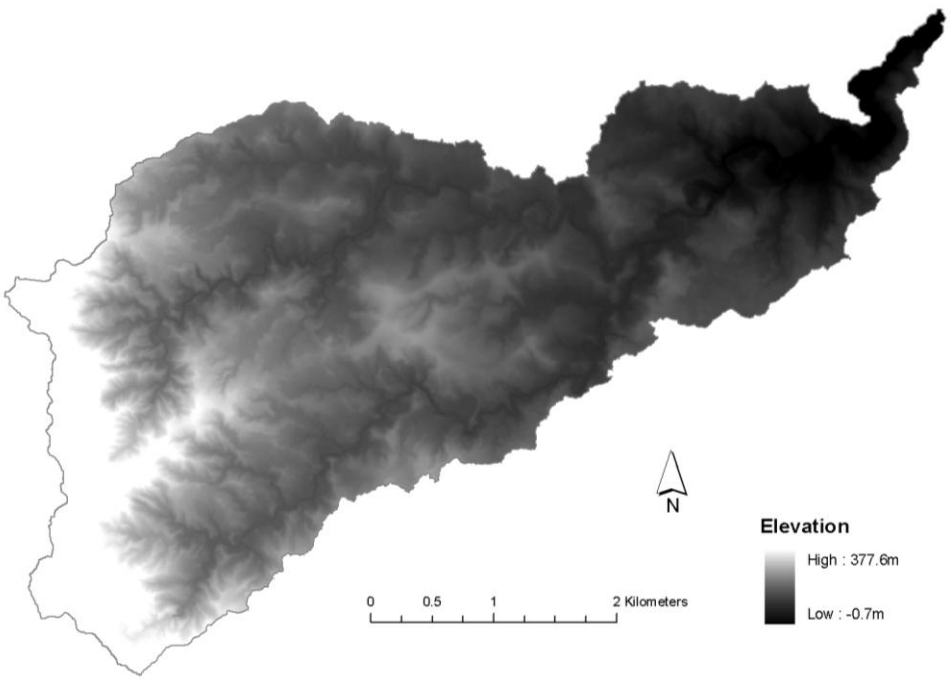

Figure 7. Elevation in Ugum Watershed.

Table 4. Elevation distribution of badlands (BL) and the entire Ugum Watershed and their proportional abundance.

ELEVATION (m)		< 50	50 - 100	100 - 150	150 - 200	200 - 250	250 - 300	300 - 350	> 350	SUM
Area (ha) (Proportion of total Area)	Ugum	134.6 (7.32%)	516.5 (28.1%)	708.7 (38.5%)	227.3 (12.3%)	109.4 (5.95%)	72.6 (3.94%)	55.4 (3.01%)	13.1 (0.71%)	1837.6 (100%)
	BL	0.3 (0.50%)	11.2 (20.3%)	31.1 (56.3%)	4.4 (7.9%)	0.6 (1.06%)	2.1 (3.78%)	4.7 (8.58%)	0.8 (1.46%)	55.2 (100%)
% BL per Category*		**0.21**	2.17	4.39	1.92	0.54	2.88	**8.57**	**6.15**	N/A
% BL in Ugum**		0.02	0.61	**1.69**	0.24	0.03	0.11	0.26	0.04	3.01

* Proportional Abundance of Badlands per Elevation Category
** Badland Cover in Ugum

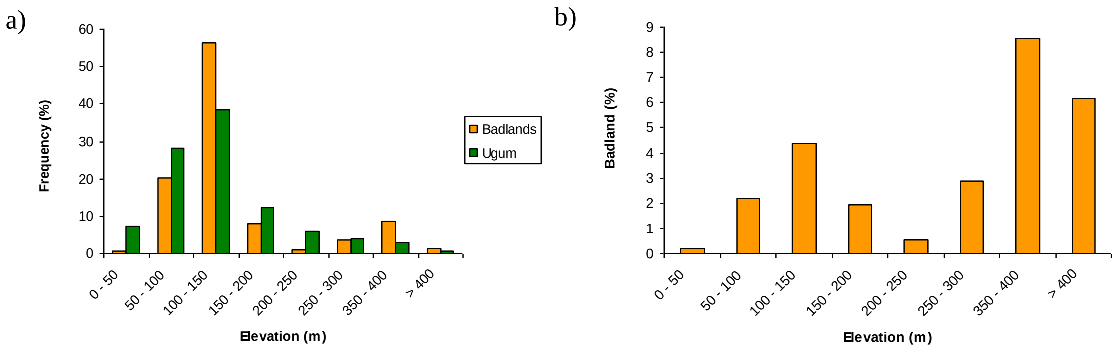

Figure 8. a. Frequency distribution of badlands and the entire Ugum Watershed per elevation categories; b. proportional abundance (percent cover) of badlands per elevation category.

<u>*Badland – Slope Relationship*</u>

Slope angles generally increase with elevation. The highest slope angles in the Ugum Watershed exceed 100 percent (Fig. 9). About half of all slopes in the watershed are less than 20 percent (Table 5, Fig.10). Most areas in Ugum Watershed including badlands have a slope of 10–20 percent. The relative abundance of badlands per elevation category increases from 2.6 percent at slopes of ≤ 10 percent to 3.5 percent at slope angle of 20–30 percent but, contrary to our expectations, gradually decreases at steeper slopes (to 1.1 % at slopes ≥ 100 %). The decrease in relative abundance of slopes less than 30 percent could be due the decreased impact of rain splashes at steeper slopes (vs. gentler slope where rain hits the soil more perpendicular).

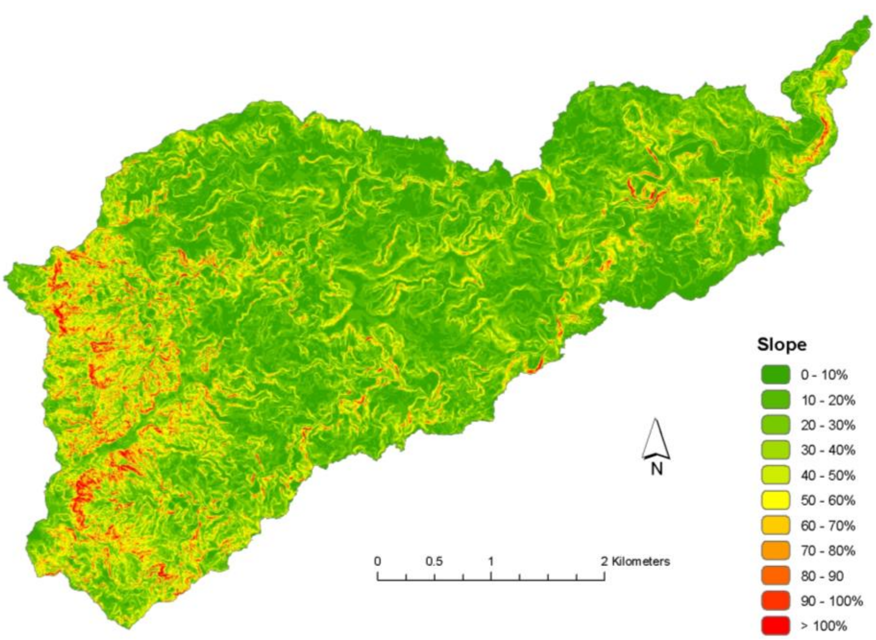

Figure 9. Slope in Ugum Watershed.

Table 5. Slope distribution of badlands and the entire Ugum Watershed and their proportional abundance.

SLOPE (%)		0-10	10- 0	20-30	30-40	40-50	50-60	60-70	70-80	80-90	90 100	> 100	SUM
Area (ha) (% of total Area)	Ugum	386.2 (21.0)	497.5 (27.1)	335.0 (18.2)	221.4 (12.1)	149.0 (8.1)	100.3 (5.5)	66.9 (3.6)	41.0 (2.2)	22.1 (1.2)	10.6 (0.6)	6.8 (0.4)	1836.8 (100.0)
	BL	10.0 (18.0)	17.0 (30.67)	11.7 (21.2)	7.2 (13.0)	4.3 (7.8)	2.4 (4.4)	1.3 (2.4)	0.8 (1.4)	0.4 (0.7)	0.2 (0.3)	0.1 (0.1)	55.3 (100.0)
% BL per Category*		2.58	3.41	**3.49**	3.25	2.90	2.41	1.97	1.90	1.76	1.69	**1.07**	N/A
% BL in Ugum**		0.54	**0.92**	0.64	0.39	0.23	0.13	0.07	0.04	0.02	0.01	< **0.01**	3.01

a)

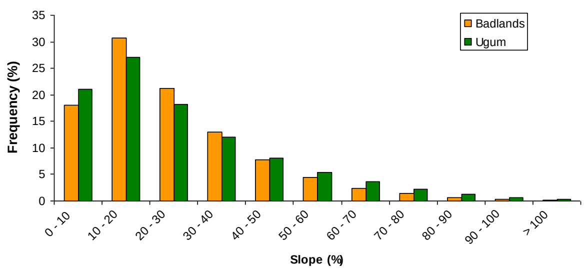

b)

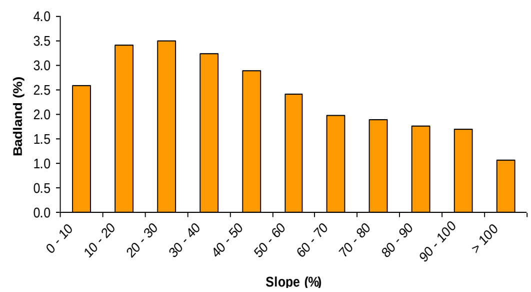

Figure 10. a. Frequency distribution of badlands and the entire Ugum Watershed per slope categories; b. proportional abundance (percent cover) of badlands per slope category.

Badland – Aspect Relationship

The aspect—the direction of a slope—in the Ugum Watershed was categorized into eight classes: north, northeast, east, southeast, south, southwest, west, and northwest (Fig. 11). Our results indicate a strong influence of aspect on badland abundance: badlands on south-east–facing slopes are about 70 percent more frequent than on north-west–facing slopes (Table 6, Fig. 12). Badland abundance decreases linearly ($R \geq 0.92$) towards northeast in both directions. This is likely due to differential wind—and hence rain—direction and sun exposure: during the wet season the island has prevailing southeast winds (or strong southwest winds during occasional monsoons) whereas during the dry season the island has prevailing trade winds, predominantly from east-northeast (Lander 2009, pers.comm.), impacting the soil more perpendicular than slopes facing other directions. Southeast to southwest-facing slopes also get more sun exposure during the dry season which dries out the soil further.

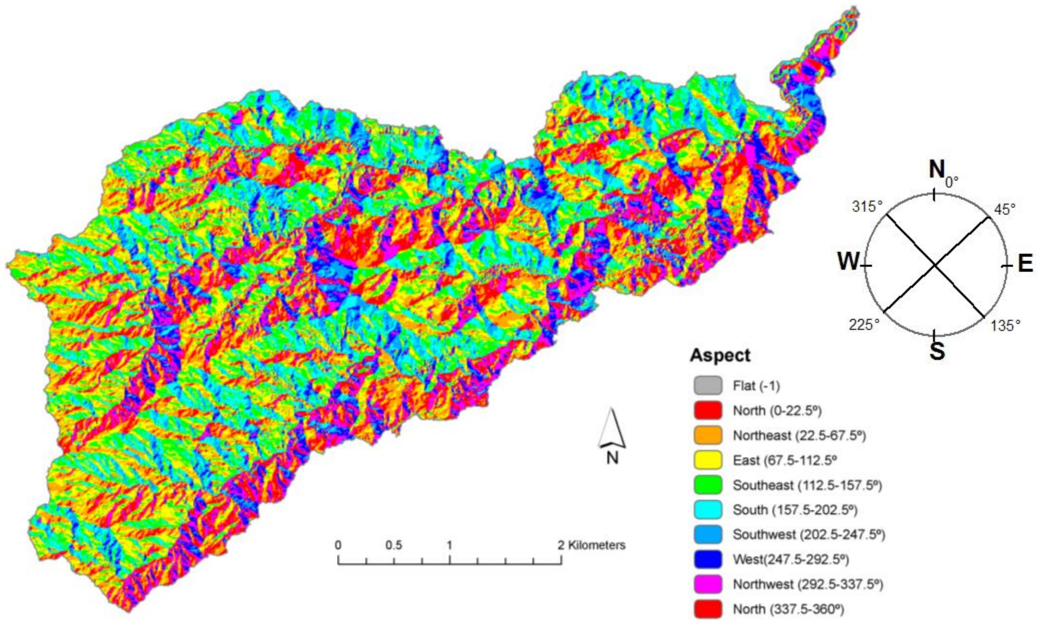

Figure 11. Aspect in Ugum Watershed.

Table 6. Aspect distribution of badlands and the entire Ugum Watershed and their proportional abundance.

ASPECT		N 337.5º - 22.5º	NE 22.5º - 67.5º	E 67.5º - 112.5º	SE 112.5º - 157.5º	S 157.5º - 202.5º	SW 202.5º - 247.5º	W 247.5º - 292.5º	NW 292.5º - 337.5º	SUM
Area (ha) (Proportion of total Area)	Ugum	254.4 (13.9)	287.9 (15.7)	295.8 (16.1)	296.5 (16.1)	230.8 (12.6)	150.8 (8.2)	134.7 (7.3)	186.8 (10.2)	1837.6 (100.0)
	BL	5.8 (10.5)	8.2 (14.8)	9.9 (17.8)	11.4 (20.6)	8.2 (14.9)	4.0 (7.3)	3.6 (6.5)	4.2 (7.6)	55.2 (100.9)
% BL per Category*		2.28	2.85	3.33	**3.83**	3.56	2.67	2.64	**2.26**	N/A
% BL in Ugum**		0.32	0.45	0.54	**0.62**	0.45	0.22	**0.19**	0.23	3.01

a) *b)*

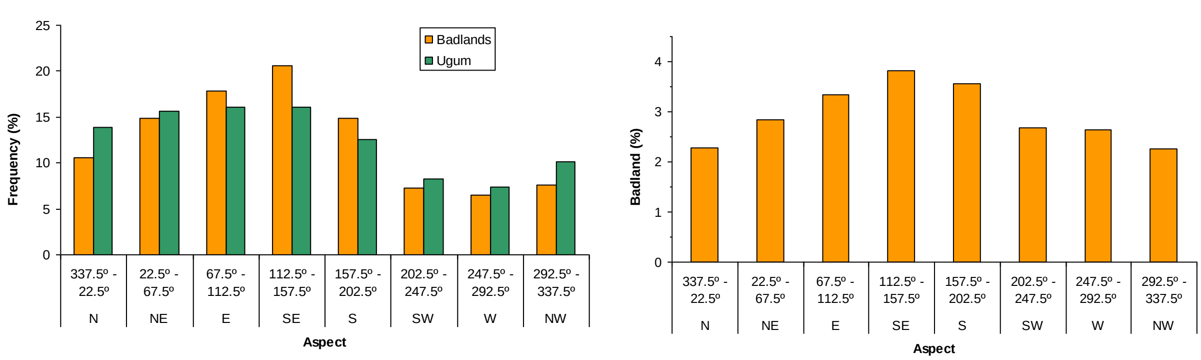

Figure 12 a. Frequency distribution of badlands and the entire Ugum Watershed per aspect categories; b. proportional abundance (percent cover) of badlands per aspect category.

Badland – Distance to Drainage Divide (DDD) Relationship

Drainage divides are ridgelines or sub-basin boundaries. Areas close to a drainage divide is generally more exposed to the elements like wind and water. The Ugum Watershed was classified into eleven sub-basins (Fig. 13). About 40 percent of all badlands are within 50 meter of a drainage divide (Table 7, Fig.14). The proportional abundance of badlands continuously decreases with increasing distance from a drainage divide. The badland cover within 50 meters of a drainage divide is twice as high (6.2 %) as the badland cover in the DDD class 50 to 100 meters (3.1 %) or any other class. These numbers clearly indicate that a higher exposure to wind and water influences badland development.

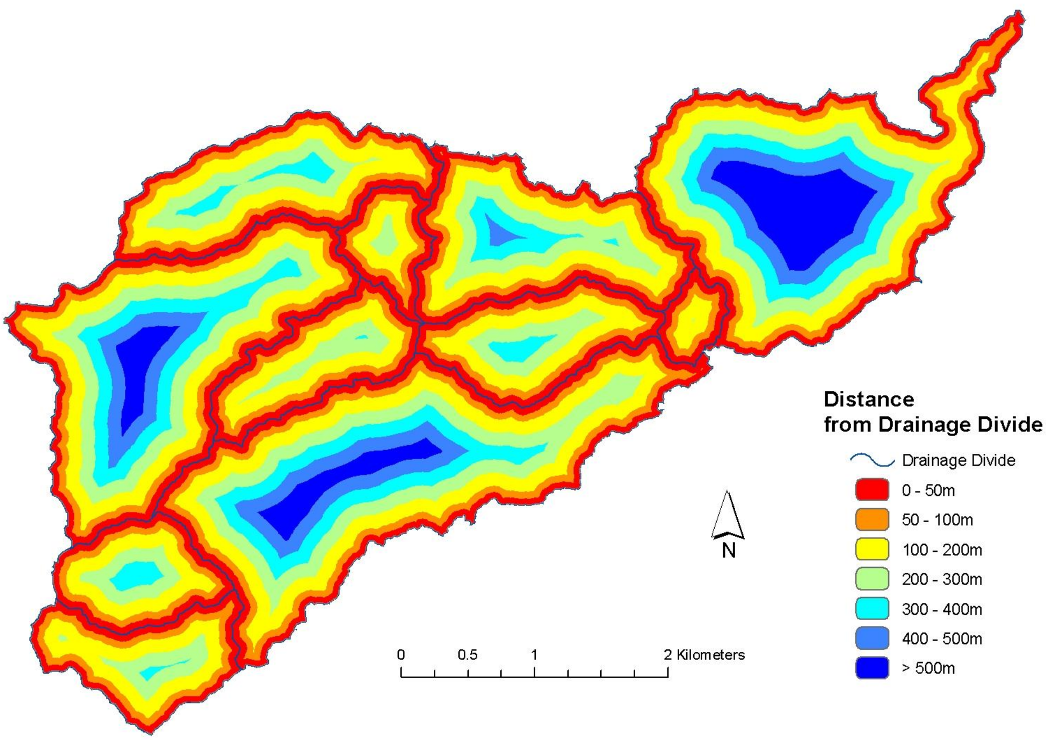

Figure 13. Distance from drainage divide in Ugum Watershed.

Table 7. Distance of drainage divide distribution of badlands and the entire Ugum Watershed and their proportional abundance.

Distance Drainage Divide (m)		0-50	50-100	100-200	200-300	300-400	400-500	>500	SUM
Area (ha) (% of total Area)	Ugum	357.4 (12.8)	294.9 (10.3)	482.7 (16.3)	326.9 (11.0)	179.5 (6.8)	105.8 (4.0)	90.6 (38.7)	1837.6 (100.0)
	BL	22.0 (39.8)	9.1 (16.5)	11.2 (20.2)	6.7 (12.1)	3.2 (5.7)	2.0 (3.7)	1.1 (2.1)	55.2 (100.0)
% BL per Category*		**6.15**	3.09	2.31	2.05	1.75	1.93	**1.25**	N/A
% BL in Ugum**		**1.20**	0.50	0.61	0.36	0.17	0.11	**0.06**	3.01

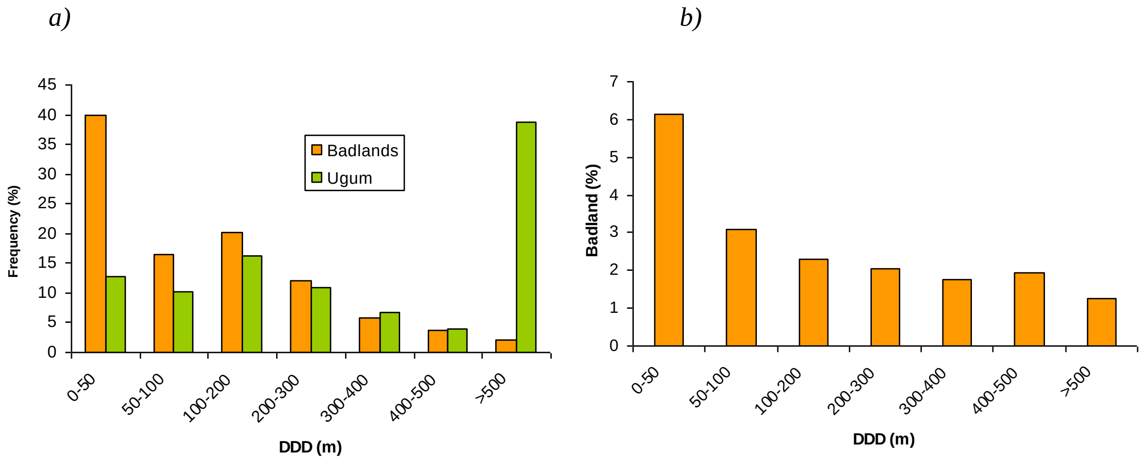

Figure 14. a. Frequency distribution of badlands and the entire Ugum Watershed per distance to drainage divide (DDD); b. proportional abundance (percent cover) of badlands per DDD category.

Badland – Geology Relationship

The majority of the Ugum Watershed is classified as volcanic rock (Fig. 15). Badlands develop on weathered volcanic rock. As expected, no badland areas were detected on limestone or in alluvium medium (Table 8, Fig.16). Most badland areas (87.2 %) are found on the Bolanos Pyroclastic Member of the Umatac Formation which covers almost the entire watershed with 89.6 percent. The remaining badlands (12.7 %) are on the Dandan Flow Member which covers 6.3 percent of the watershed. However, the proportional abundance of badlands in the Dandan Flow Member is more than twice as high compared to the Bolanos Pyroclastic Member.

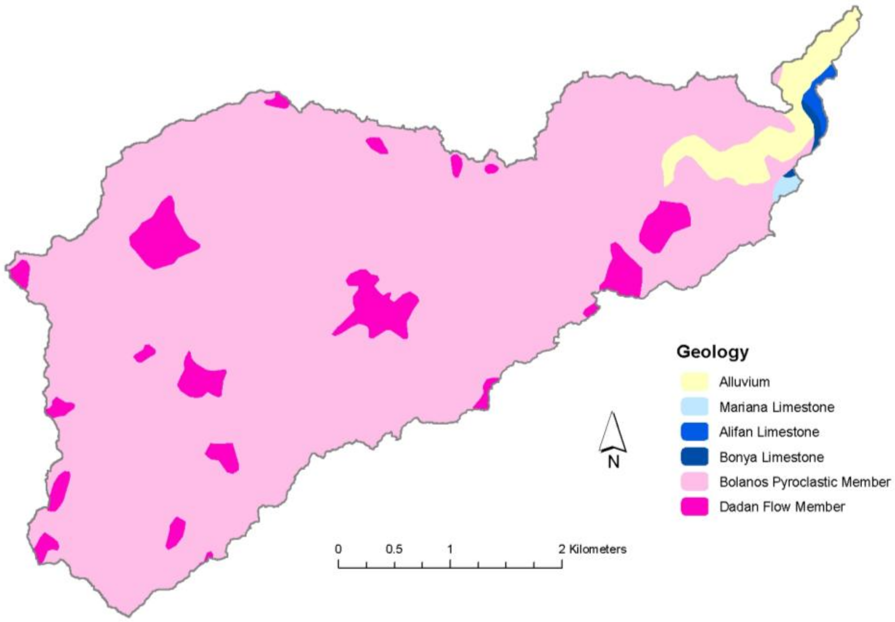

Figure 15. Geology of Ugum Watershed.

Table 8. Geology distribution of badlands and the entire Ugum Watershed and their proportional abundance.

GEOLOGIC UNIT		Qal[1]	Qtma[2]	Tal[3]	Tb[4]	Tub[5]	Tud[6]	SUM
Area (ha) (% of total Area)	Ugum	63.9 (3.5)	3.7 (0.2)	6.1 (0.3)	3.4 (0.2)	1645.6 (89.6)	114.9 (6.3)	1837.6 (100.0)
	BL	<< 0.01 (<<0.1)	-	-	-	48.2 (87.2)	7.0 (12.7)	55.2 (100.0)
% BL per Category*		0.04	-	-	-	2.93	**6.13**	N/A
% BL in Ugum**		< 0.01	-	-	-	**2.62**	0.38	3.01

[1] Alluvium, [2] Mariana Limestone, [3] Alifan Limestone, [4] Bonya Limestone, [5] Bolanos Pyroclastic Member, [6] Dadan Flow Member

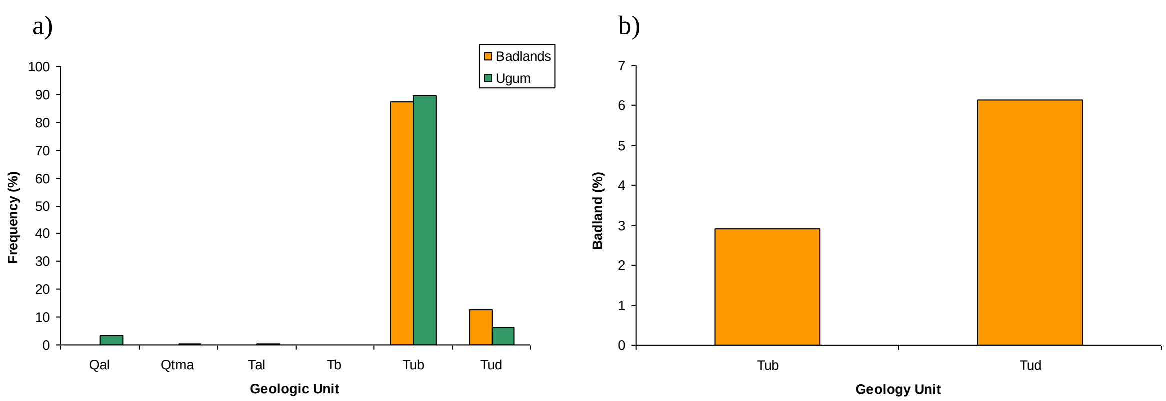

Figure 16. Frequency distribution of badlands and the entire Ugum Watershed per geologic unit; b. proportional abundance (percent cover) of badlands per geologic unit (legend for geologic units see Table 8).

Badland – Soil Relationship

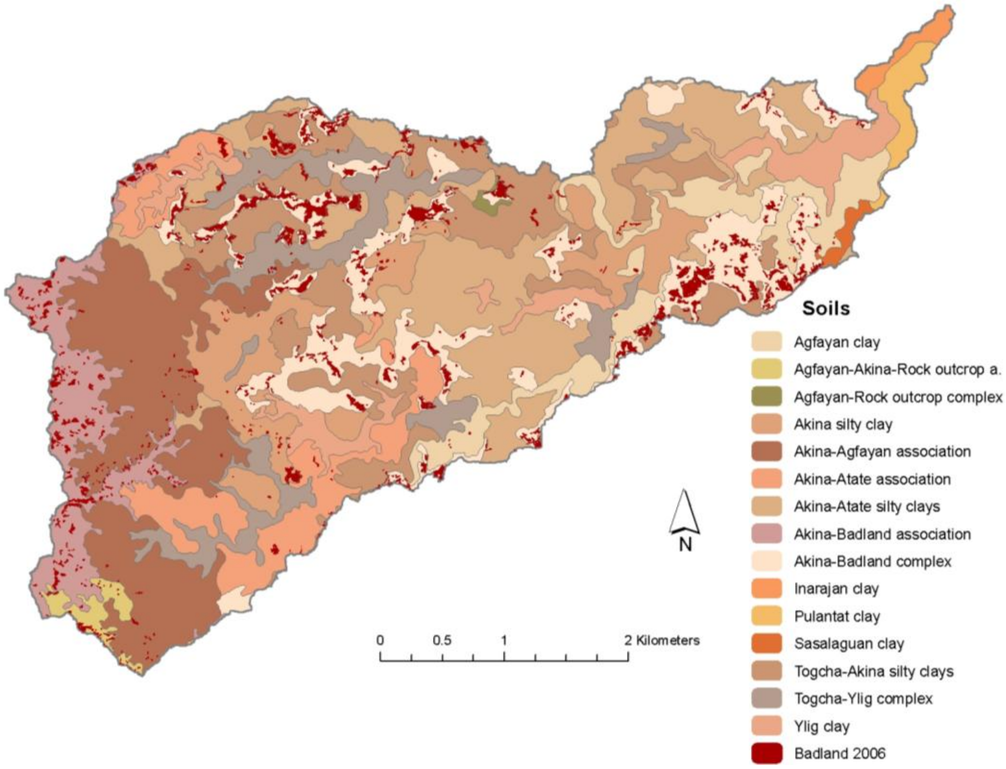

Figure 17. Soils of Ugum Watershed.

As expected, by far the most badlands are found in soils classified as the Akina-Badlands complex (Fig. 17); within that complex 47.1 percent have slope of 15–30 percent, 11.7 percent have a slope of 7–15 percent, and 6.4 percent have a slope of 30–60 percent (Table 10, Fig. 18). Another 13.7 percent of all badlands are located on the Akina-Badlands association with steep slopes. A smaller percent of badlands (4.4 %) is on Togcha-Akina silty clays with 7%–15% slopes. All other soil categories found in the watershed, except the Pulantat, Inarajan, and Agfayan clay, have only a few badlands (≤ 2.6 %). Proportional abundance of badlands is also highest in the Akina-Badlands complex with 19.4 percent, 16.6 percent, and 12.9 percent for slopes of 7–15 percent, 30–60 percent, and 15–30 percent, respectively.

Table 9. Statistical breakdown of badland distribution in regards to soil.

SOIL CATEGORY	Area (ha) (% of total Area)		Proportional Abundance of BL per Category (%)	BL in Ugum (%)
	Ugum	Badlands		
Agfayan-Akina-Rock outcrop association, extremely	18.8 (1.0)	0.9 (1.7)	5.0	0.05
Agfayan clay, 30% to 60% slopes	111.6 (6.1)	0.3 (0.6)	0.3	0.02
Agfayan-Rock outcrop complex, 30% to 60% slopes	2.9 (0.2)	0.0 (0.1)	1.4	0.00
Akina-Agfayan association, steep	262.9 (14.3)	0.9 (1.6)	0.3	0.05
Akina-Atate association, steep	124.4 (6.77)	1.2 (2.3)	1.0	0.07
Akina-Atate silty clays, 7% to 15% slopes	43.1 (2.3)	0.4 (0.7)	0.9	0.02
Akina-Atate silty clays, 30% to 60% slopes	92.5 (5.0)	1.4 (2.6)	1.5	0.08
Akina-Atate silty clays, 15% to 30% slopes	171.2 (9.3)	0.7 (1.3)	0.4	0.04
Akina silty clay, 3% to 7% slopes	6.7 (0.4)	-	0.0	0.00
Akina silty clay, 7% to 15% slopes	36.1 (2.0)	0.2 (0.4)	0.6	0.01
Akina silty clay, 15% to 30% slopes	69.8 (3.8)	1.3 (2.4)	1.9	0.07
Akina silty clay, 30% to 60% slopes	29.1 (1.6)	0.1 (0.2)	0.4	0.01
Akina-Badland association, steep	**123.0 (6.7)**	**7.6 (13.7)**	**6.2**	**0.41**
Akina-Badland complex, 7% to 15% slopes	**33.3 (1.8)**	**6.5 (11.7)**	**19.4**	**0.35**
Akina-Badland complex, 15% to 30% slopes	**201.8 (11.0)**	**26.0 (47.1)**	**12.9**	**1.42**
Akina-Badland complex, 30% to 60% slopes	**21.2 (1.2)**	**3.5 (6.4)**	**16.6**	**0.19**
Inarajan clay, 0% to 4% slopes	12.5 (0.7)	-	0.0	0.00
Pulantat clay, 15% to 30% slopes	4.7 (0.3)	-	-	0.00
Pulantat clay, 30% to 60% slopes	18.4 (1.0)	-	-	0.00
Sasalaguan clay, 7% to 15% slopes	7.5 (0.4)	0.0 (<0.1)	0.2	0.00
Togcha-Akina silty clays, 3% to 7% slopes	34.0 (1.9)	1.1 (2.0)	3.2	0.06
Togcha-Akina silty clays, 7% to 15% slopes	186.9 (10.2)	2.4 (4.4)	1.3	0.13
Togcha-Ylig complex, 7% to 15% slopes	54.2 (3.0)	0.1 (0.2)	0.2	0.00
Togcha-Ylig complex, 3% to 7% slopes	83.3 (4.5)	0.4 (0.8)	0.5	0.02
Ylig clay, 3% to 7% slopes	87.6 (4.8)	0.1 (0.1)	0.1	0.00
SUM	1837.6 (100.0)	55.2 (100.0)	N/A	3.01

a)

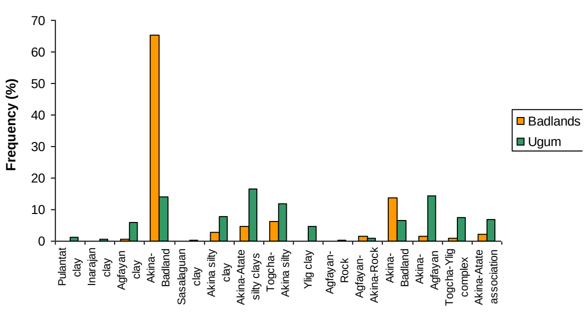

b)

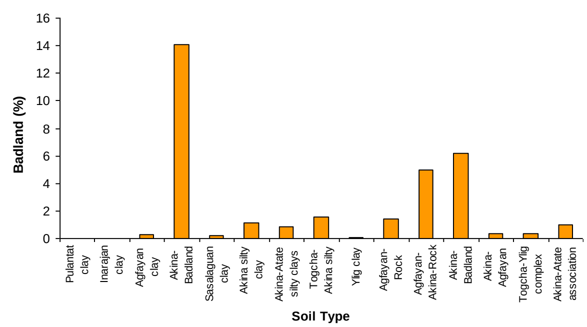

Figure 18. Frequency distribution of badlands and the entire Ugum Watershed per soil unit; b. proportional abundance (percent cover) of badlands per soil unit.

Summary of Significance Test

A Chi Square Test for Proportions was performed to test the difference of the distribution of terrain attributes of badlands and the entire Ugum Watershed to see if the terrain attributes of badlands is significantly different than the terrain attributes of the watershed (Table 10). The distribution of badlands in specific categories of elevation, slope, distance to drainage divide (DDD), and soil is significantly different ($p < 0.0001$) to the entire watershed; hence, the results suggest that these terrain attributes have a significant influence on badland occurrence.

Table 10. Significance of differences of terrain attributes of badlands compared with terrain attributes of entire Ugum Watershed.

	ELEVATION	ASPECT	SLOPE	DDD	GEOLOGY	SOIL
$\chi 2$	33.45	3.52	66.02	96.55	10.9	85.00
df	7.00	7	12	6	5	14
Crit. Value for .05	14.10	14.1	21.03	12.59	11.070	23.69
P-value	**<0.0001***	0.833	**< 0.0001***	**< 0.0001***	0.053	**< 0.0001***

* highly significant at < 0.0001 level

SUMMARY & CONCLUSION

We analyzed the extent of badlands in 1946 and 2006 in a study area within the Ugum Watershed. Our results show that badlands are dynamic. Almost 40 percent of today's badlands have developed over the last 60 years. Some badlands also disappeared, but the exact number could not be determined because of inherent characteristics of the 1946 aerial photo.

We also examined the effect of topography on badland occurrence in the Ugum Watershed. Our results suggest a significant relationship of badland occurrence with elevation, slope, distance to drainage divide, and soil, but not with geology or aspect. The conclusions drawn here need to be confirmed for other areas in southern Guam so that results can be used more reliable to model potential badland areas.

RECOMMENDATIONS

This study provided valuable reconnaissance information regarding badland changes over time. However, we were only able to look the extent of badlands in two years (1946 and 2006). A more extent and finer time-scale will produce more evidence on the rate of change as well as inter-decadal variances.

A comparison of the structural pattern of badland patches of 1946 and 2006 would provide an insight of how badland patches change over time; *e.g.*, can we see an increase in number of patches or does the mean patch size change. This analysis was based on only the 2006 badland patches we digitized. The badlands in 1946 were not analyzed this way due to their poor quality and their pixel.

Re-vegetation is an important measure to stop or at least slow erosion processes. By identifying younger badlands in our study, future research could use this information to test whether younger badlands have a better ability to be re-vegetated because they might not have fully eroded to the bedrock. Understanding more about badland behavior is essential to better manage them. Therefore, more research needs to be directed toward these highly erodible surfaces.

REFERENCES

Bell, F.; Falanruw, M.; Lawrence, B.; Limtiaco, D.; Nelson D. 2002. Draft vegetation strategy for southern Guam. Honolulu, HI: U.S. Department of Agriculture, Forest Service; U.S. Department of Agriculture, Natural Resources Conservation Service, Government of Guam Division of Forestry.

Bewket, W. 2002. Land Cover Dynamics Since the 19502 in Chemoga Watershed, Blue Nile Basin, Ethiopia. Mountain Research and Development 22(3):263–269.

Calzolari, C., and Ungaro, F., 1998. Geomorphic Features of a Badland (biancana) Area (Central Italy): characterization, distribution and quantitative spatial analysis. Catena 31:237–256.

Cantón, Y., Del Barrio, G., Solé-Benet, A., Lázaro, R. 2004. Topographic controls on the spatial distribution of ground cover in the Tabernas badlands of SE Spain. Catena 55:341–365.

Capone, M., 2009. Personal communication. Guam National Park Service.

Carter, J. 2009. Putting the Pacific Island on the National Map – Overview of Coastal Change Analysis Program (C-CAP). Presentation 16 March 2009 for Government on Guam. National Oceanic and Atmospheric Administration *(*NOAA) Pacific Services Center.

Clark, M. L., Rendell, H. M. 2006. Process-form relationships in Southern Italian badlands: erosion rates and implications for landform evolution. Earth Surface Processes and Landforms 31: 15-29.

Donnegan, Joseph A.; Butler, Sarah L.; Grabowiecki, Walter; Hiserote, Bruce A.; Limtiaco, David. 2004. Guam's forest resources, 2002. Resour.Bull. PNW-RB-243. Portland, OR: U.S. Department of Agriculture, Forest Service, Pacific Northwest Research Station.

Endress, B.A., Chinea, J.D. 2001: Landscape Patterns of Tropical Forest Recovery in the Republic of Palau. Biotropica 33(4): 555–565.

Golabi, M. H., Iyekar, C., Minton, D., Raulerson, C. L., Chargualaf Darke 2005. Watershed Management to Meet Water Quality Standards by Using the Vetiver System in Southern Guam. AU J.I. 9(1): 64-70???

Khosrowpanah, S., Jocson, J. 2005. Environmental Assessment for Non-Point Sources of Pollution for Ugum Watershed. Technical Report No. 109, Water and Environmental Research Institute, University of Guam.

Khosrowpanah, S., Heitz, L. F., Wen, Y., Park, M. 2007. Developing a GIS-based Soil Erosion Model of Ugum Watershed. Technical Report No. 117, Water and Environmental Research Institute, University of Guam.

Khosrowpanah, S., Wen, Y., Jocson, J., and Taborosi, D., 2008. Natural Resources Atlas of Southern Guam. Technical Report No. 124, Water and Environmental Research Institute, University of Guam.

Kottermair, M., and Olsen, A., unpublished. Typhoon Atlas of Micronesia 1945 – 2007.

Lander, M.A., 2009. Oral communication. Water and Environmental Research Institute , University of Guam.

Lander, M.A., Guard, C.P. 2003. Creation of a 50-year rainfall database, annual rainfall climatology, and annual rainfall distribution map for Guam. Technical Report No.102, Water and Environmental Research Institute, University of Guam.

Lander, M.A. 1994. Meteorological factors associated with drought on Guam. Technical Report No.75, Water and Environmental Research Institute, University of Guam.

Levesque, L.M., 2000: Investigating Landscape Change and Ecological Restoration: An Integrated Approach Using Historical Ecology and GIS in Waterton Lakes National Park, Alberta. MASTER OF SCIENCE in Interdisciplinary Studies. School of Environmental Studies Department of Geography. University of Guelph.

Lewis. R.R. 1999. Quantifying geomorphic processes of Guam's Taelayag River badlands by determining rates for basin yield, slope retreat and fracture movement. Master's thesis, University of Guam, Guam

Liberti M., Simoniello T. Carone M., Coppola R., D'Emilio M., Lanfredi M., Macchiato M. 2006. Badlands Area Mapping from LANDSAT-ETM Data, Proceedings of the 2nd Workshop of the EARSeL SIG on Land Use and Land Cover. Center for Remote Sensing of Land Surfaces, 434–440.

Lin, Z., Ogushi, T. 2004. Drainage density, slope angle, and relative basin position in Japanese bare lands from high-resolution DEMs. Geomorphology 6:159–173.

Lobban, C. S., Schefter, M. 1997. Tropical Pacific Island Environments. University of Guam Press, p.128–141.

Moretti, S., Rodolfi, G. 2000. A typical "calanchi" landscape on the Eastern Apennine margin (Atri, Central Italy): geomorphological features and evolution. Catena 40: 217–228.

Natural Resource Conservation Service (NRCS), 1996. Ugum Watershed Management Plan, Territory of Guam. U.S. Department of Agriculture, Hagåtña, Guam.

Natural Resource Conservation Service (NRCS), 2001. Fena Watershed Resource Assessment: Erosion and Sediment Identification for critical Area Treatment, Territory of Guam. U.S. Department of Agriculture, Hagåtña, Guam.

Natural Resource Conservation Service (NRCS), 2006. Preliminary GIS Erosion Estimates for Cetti and Sella Watersheds. U.S. Department of Agriculture, Natural Resources Conservation Service, Pacific Islands Area.

Rinehart, A. 1995. Reconnaissance Botanical Survey of the Ugum Riverine Forest. University of Guam Herbarium Contribution No. 30, 63 pages.

Scheman N., 2002 M.S. thesis on Identification of Erosion Process and Sources of Exposed Patches in the La Sa Fua Watershed of Southern Guam. WERI, University of Guam.

Siegrist, H.G. Jr, Denton G., Heitz L., et al. 1996. Wetlands resources in the Ugum Watershed, Guam. A general description and preliminary functional assessment of palustrine-riverine wetland system. Technical Report No. 76, Water and Environmental Research Institute, University of Guam.

Torri, D., Colica, A. Rockwell, D. 1994. Preliminary study of the erosion mechanisms in a *biancana* badland (Tuscany, Italy). Catena 23: 281-294.

Tracey, J.I.Jr., Schlanger, S.O., Stark, J.T., Doan, D.B., May, H.G., 1964: General Geology of Guam – Geology and Hydrology of Guam, Mariana Islands. Geological Survey Professional Paper, 403-A

Wen, Y., Khosrowpanah, S., and Heitz, L.F.. 2009. Watershed Land Cover Change in Guam. Technical Report No. 124. Water and Environmental Research Institute, University of Guam.

WPC (Watershed Planning Committee) 1999. Ugum Watershed Restoration Strategy. Strategy developed by subgroup of WPC, Guam.

Young, F.J. 1988. Soil Survey of Territory of Guam. USDA Soil Conservation Service.